

Numerical Technique of Flow Heat through Various Configurations of Steel Shapes

Abbas Zghair Salman, Roshen Tariq Ahmed

Energy and Renewable Energies Technology Center, University of Technology, Baghdad, Iraq-10066

Abstract— A numerical study of heat transfer through various configuration Of steel shapes are studied in details. The base surface of the shape is assumed at uniform base temperature, while the other surfaces are exposed to natural convection. The governing equations for conduction in the steel section shape are written in finite difference form and are solved numerically by using an iterative technique coupled with the natural convection boundary conditions. The effect of changing the temperature difference (between base and ambient), inclination angle and aspect ratio on the temperature and heat flow distributions and total heat transfer from the shape is studied in details. The results show that the total heat transfer increases as the temperature difference increases and as the aspect ratio decreases. It also increases as the inclination angle increases $0 \leq \theta \leq \pi$ except when $\theta = \pi/2$ and $\theta = \pi$. Under the same conditions, L-shape has the highest overall heat transfer coefficient and the lowest one is T-shape. General correlations in the range of the studied parameters are given. They help the designers to calculate simply the total heat transfer from different shapes of steel structure at different operating and geometrical conditions.

Keywords— Heat transfer, Numerical analysis, Heat flow.

I. INTRODUCTION

The steel sections (I, L, U and T) are: widely used in the heat transfer industrial equipment, e.g. furnaces and aluminum reduction cells. Most of the designers used its strength as a basis of selection. They have different heat transfer characteristics whenever efficient and homogeneous cooling or heating are required.

Hence, if the strength requirements me achieved by wing different shapes, the designer has to select the better shape from the beat-transfer point of view. That is why this study was done, to give the designers the tools to deal with the beat transfer characteristics of the different steel structure shapes (L, U and T).

In aluminum reduction cells, the side wall ledge profile is depending on the cell design. Particular cell geometry and operating parameters affect the cell fluid dynamics and heat transfer. A properly designed cell will have a desirable heat distribution and suitable steady-state ledge profile. It helps to maintain a stable metal pad and therefore allows stable cell operation and high current efficiency [1]. A numerical and experimental study was performed to predict the heat transfer from I-beams having different operating and geometrical conditions. The temperature distribution and effectiveness were reported for each case. Its finite difference results agreed fairly with its experimental results [2]. Moreover, these results were checked by using the finite element computer package "FEHT"[3]. The difference between both numerical results was 2% [4].

Several two-dimensional studies were performed to determine the natural convection from L-shaped corners under different conditions. However, these studies were restricted to the fluid flow and beat transfer near the corner; they did not take the conduction inside the L-shape into consideration [5].

In the present work, the heat transfer from different steel structure shapes (L, U and T) was studied. The analysis starts with the conduction from the base of the shape to its surfaces and ends with natural convection to the air- Figure 1 shows the L-shape geometry and the values of the studied parameters. The used natural convection correlations from different hot surfaces (with different facings and inclinations) were extracted from the literature as follows:

1- Natural convection from vertical surfaces.

$$Nu = 0.68 + \frac{0.67Ra^{0.25}}{\left(1 + \left(\frac{0.492}{Pr}\right)^{9/16}\right)^{4/9}}, \quad Ra < 10^9 \quad (1)$$

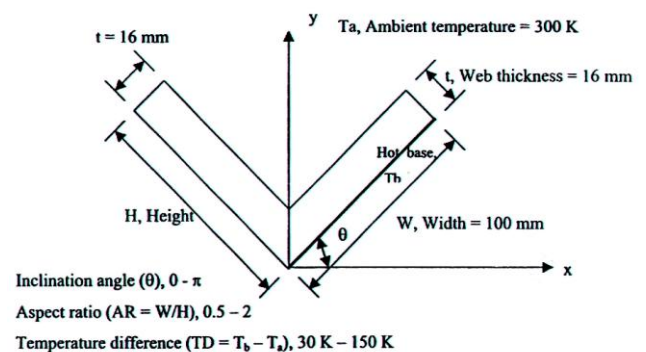


Fig. 1. L-shape geometry.

2- Natural convection from hot horizontal surface facing upward [10]

$$Nu = 0.54Ra_a^{0.25}, \quad 2 \times 10^4 < Ra < 8 \times 10^6 \quad (2)$$

$$Nu = 0.15Ra_a^{0.3333}, \quad 8 \times 10^6 < Ra < 8 \times 10^{11} \quad (3)$$

3- Natural convection from hot horizontal surface facing downward [11, 12]

$$Nu = 0.27Ra_a^{0.25}, \quad 10^5 < Ra < 10^{11} \quad (4)$$

In the above Eqs. (1-4), all the properties in the dimensionless groups, are evaluated at $T_f = (T_w - T_a)/2$, and β is equal to $1/T_f$. The height of the vertical surface and the width of the horizontal surface were taken as a characteristic length, in each case.

4- Natural convection from hot inclined surface [6]

a) Facing downward:

$$Nu = 0.54(Gr Pr \cos \theta_v)^{0.25}, \theta_v < 88^\circ \quad (5)$$

b) Facing upward:

$$Nu = 0.14[(Gr Pr)^{0.3333} - (Gr_c Pr)^{0.3333}] + 0.56(Gr Pr \cos \theta_v)^{0.25}, \quad 15^\circ \leq \theta_v \leq 75^\circ \quad (6)$$

Where, θ_v , is the angle, which the inclined surface makes with the vertical axis.

The quantity Gr_c is a critical Grashof number and it depends on the orientation angle (θ_v), according to the data of table I. For $Gr < Gr_c$ the first term of Eq. (6) is dropped out Both Eqs. (5 and 6) are valid in the range of $10^5 < Gr Pr \cos \theta < 10^{11}$ and all properties are evaluated at $T = T_w - 0.25(T_w - T_a)$, except A which equals $1/T_f$. The characteristic length is the length of the inclined surface.

TABLE I. Critical Grashof number of Eq. (6) for various orientation angles.

θ_v	15°	30°	60°	75°
Gr_c	5×10^9	2×10^9	10^8	10^6

II. NUMERICAL ANALYSIS

The general equation of conduction heat transfer, under the assumption of two-dimensional heat flow, steady state with no heat generation and constant thermal conductivity, is expressed as follows:

$$\frac{\partial^2 T}{\partial x^2} + \frac{\partial^2 T}{\partial y^2} = 0 \quad (7)$$

The numerical solution of this equation using specified boundary conditions predicts the heat flow and temperature distribution in the solution domain. Using the finite-difference approach, the continuous domain is discretized, so that the dependent variables are considered to exist only at discrete points. Derivatives are approximated by differences resulting in an algebraic representation of the above partial differential equation. Hence the solution domain must be divided into mesh or grid, as shown in Fig. 2. Different simulations [7] of the above partial differential equation lead to:

$$\frac{T_{m+1,n} + T_{m-1,n} - 2T_{m,n}}{(\Delta x)^2} + \frac{T_{m,n-1} + T_{m,n+1} - 2T_{m,n}}{(\Delta y)^2} = 0 \quad (8)$$

This equation is valid for interior nodes. For surface nodes and comers nodes (which is posed to convection boundary conditions, see Figs. (1-2), the following equations are applied [8]:

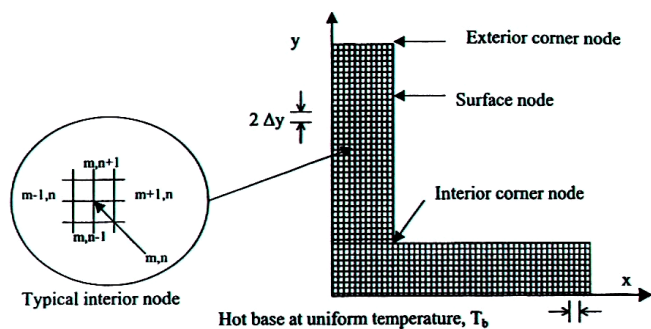


Fig. 2. Schematic diagram of the solution domain of the L-shape.

a) for surface node.

$$k\Delta y \frac{T_{m,n} - T_{m-1,n}}{\Delta x} + k \frac{\Delta x}{2} \frac{T_{m,n} - T_{m,n-1}}{\Delta y} + k \frac{\Delta x}{2} \frac{T_{m,n} - T_{m,n+1}}{\Delta y} + h\Delta y(T_{m,n} - T_a) = 0 \quad (9)$$

b) for exterior corner node

$$k \frac{\Delta y}{2} \frac{T_{m,n} - T_{m-1,n}}{\Delta x} + k \frac{\Delta x}{2} \frac{T_{m,n} - T_{m,n-1}}{\Delta y} + h_k \frac{\Delta x}{2} (T_{m,n} - T_a) + h_v \frac{\Delta x}{2} (T_{m,n} - T_a) = 0 \quad (10)$$

c) for interior corner node

$$k\Delta y \frac{T_{m,n} - T_{m-1,n}}{\Delta x} + k \frac{\Delta y}{2} \frac{T_{m,n} - T_{m,n-1}}{\Delta x} + h\Delta x \frac{T_{m,n} - T_{m,n-1}}{\Delta y} + k \frac{\Delta x}{2} \frac{T_{m,n} - T_{m,n+1}}{\Delta y} + h_h \frac{\Delta x}{2} (T_{m,n} - T_a) + h_v \frac{\Delta y}{2} (T_{m,n} - T_a) = 0 \quad (11)$$

If any surface is insulated, Eq. (9-11) can be used but h must be set equal to zero.

Writing the suitable equation for each node in the solution domain (Fig. 2) will lead to n linear algebraic equations in n unknowns. It may be solved by using matrix algebra. When the number of nodes is very large, an iterative technique may frequently yield a more efficient solution to the nodal equations than a direct matrix inversion [9-10]. In the present work Gauss-Siedel iterative technique is applied to get the temperature distribution inside the solution domain as follows:

- 1- Assume initial values of T_i
- 2- Calculate new values of T_i by using Eqs.(8-11) and the appropriate boundary conditions.
- 3- Repeat step 2 until convergence takes place, viz. when successive iteration differs by very small amount $|T_{i\text{new}} - T_{i\text{old}}| \leq 0.01 \text{ K}$.

In each iteration by using Equations (8-11) a new heat transfer coefficient at different surfaces and corners nodes is calculated (as it depends on the surface temperature). The boundary conditions of the outer surfaces may be classified as follows:

- 1- The base surface is isothermal surface (uniform base temperature).
- 2- Other surfaces are exposed to natural convection; it may be vertical wall, heated horizontal wall facing upward or downward and heated inclined wall facing upward or downward. The used correlations in the present work were stated in the previous section. The surface radiation is not considered in the present analysis.

Finally, the heat transfer coefficients and the temperature distribution are predicted numerically. Hence, the total heat transfer (Q) from the steel structure shape per unit length in the third direction, the effectiveness (ϵ) and the overall heat transfer coefficient (U) can be expressed as follows [11-14]:

$$Q = \sum_{i=1}^n h_i A_i (t_i - t_a) \quad (12)$$

$$\epsilon = \frac{Q}{Q_b} \quad (13)$$

$$U = Q / (A_b (t_b - t_a)) \quad (14)$$

Where:

n= is the number of nodes on the surfaces exposed to convection.

Q_b is the heat transfer from the base without the steel structure.

Shape per unit length in the third direction = $h_b \times A_b \times (t_b - t_a)$

The grid fineness was a compromise between accuracy and computational time. That is why, a grid independence study was conducted- It was carried out by increasing the number of grids in both x and y directions. The suitable number of mesh nodes was chosen when the change in overall heat transfer coefficient becomes negligible. Increasing the number of nodes beyond this value increases the computation time without appreciable change in the results [15-17].

III. RESULTS AND DISCUSSIONS

The present numerical model and associated computer program were designed to study different shapes (L, U and T) having uniform base temperature and different operating and geometrical conditions. However, the reported results and correlations were made within the following ranges:

- 1- Inclination angles for L-shape having AR=1 are 0, $\pi/6$, $\pi/3$, $\pi/2$, $2\pi/3$, $5\pi/6$ and π (see Fig. 1).
- 2- Aspect ratios for L-shape having $\theta=0$ are 0.5, 1 and 2.
- 3- U-shape and T-shape having $\theta=0$ and π .

In each of the above cases the temperature difference between the uniform base and ambient temperature was varied from 30 K to 150 K. The other parameters are assumed to be constant ($T_a=300$ K, $k=60.5$ W/m K, $W=100$ mm and $t=16$ mm). While the shape width is constant, its height depends on the aspect ratio [18-19].

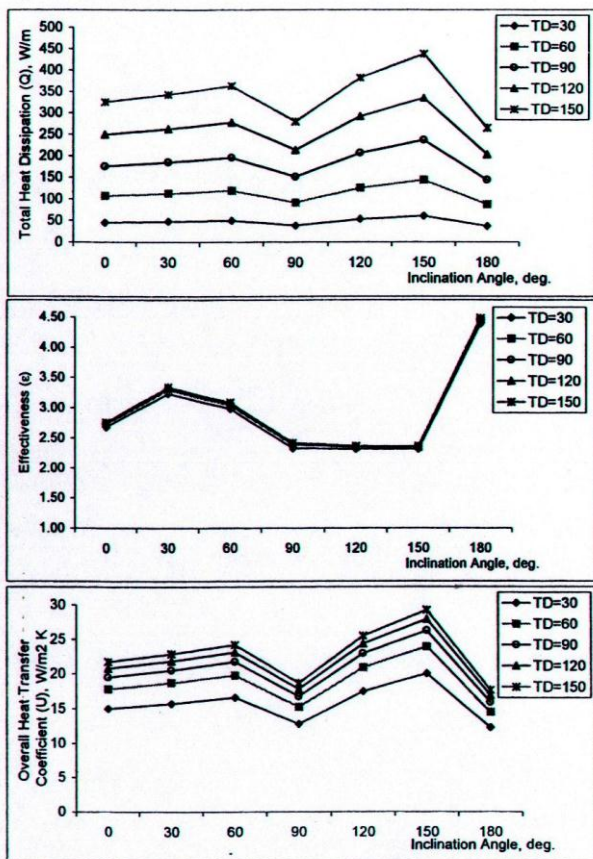


Fig. 3. Effect of inclination angle for different temperature difference (TD, K)

A. Effect of Inclination Angle, for L-shape having AR=1

For different temperature difference (TD), Fig. 3 shows the effect of the inclination angle (θ) on the total heat dissipation (Q), effectiveness (ϵ) and overall heat transfer coefficient (U). This figure shows that as TD increases both Q and U increase (as expected). However, ϵ changes slightly with TD variation. It is clear from this figure that as θ increases Q and U increase except at $\theta=\pi/2$ and π where they have lowest heat transfer rates.

L-shape surfaces are hot surfaces facing downward. Which have smallest heat transfer coefficient compared with other hot surfaces. The effectiveness varied from about 2.25 at $\theta=\pi/2$, $2\pi/3$ and $5\pi/6$ to 4.5 at $\theta=\pi$. The temperature distributions for selected inclination angles are shown in Fig. 4. It is clear that the heat flow in the unheated web (vertical web when $\theta = 0$) is almost one-dimensional.

Simplified engineering correlation is given for each case by using curve-fitting technique. The used equation, which is familiar in engineering applications, is:

$$U = a\Delta t^b \tag{15}$$

The constants a and b depend on the inclination angle, as shown in table II.

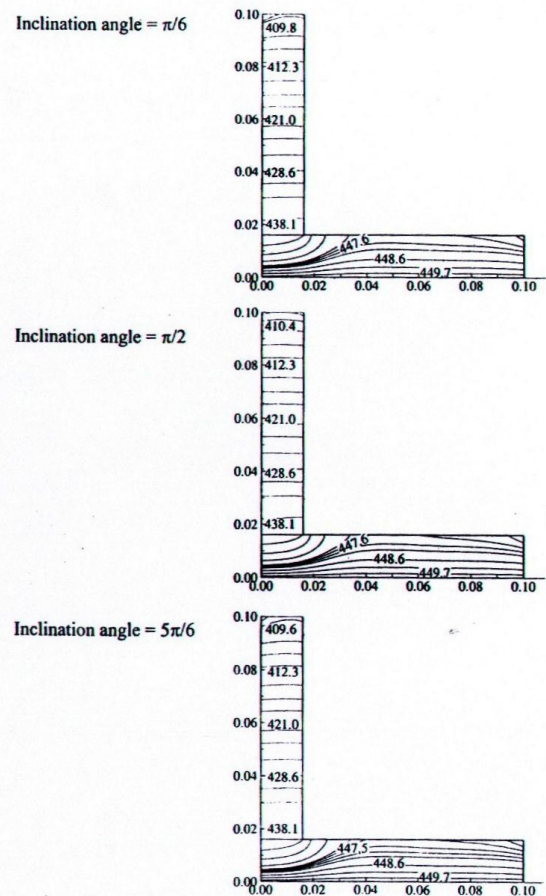


Fig. 4. Temperature contours across L-shape sections for different inclination angles (AR=1, TD=150 K, $T_b=450$ K, $T_a=300$ K, $k = 60.5$ W/m K, $W=H= .1$ m & $t=.016$ m).

TABLE II. Constants of Eq. (15) for various inclination angles (θ).

θ	a	b
0	6.9	0.23
$\pi/6$	7.25	0.23
$\pi/3$	7.68	0.23
$\pi/2$	5.91	0.23
$2\pi/3$	8.08	0.23
$5\pi/6$	9.26	0.23
π	5.62	0.23

B. Effect of Aspect Ratio, for L-shape having $\theta=0$

Figure 5 shows that as the aspect ratio decreases the total heat dissipation, effectiveness and overall heat coefficient increase because as AR decreases the shape height increases, hence the total surface area of the shape increases, consequently, Q increases. The same effect of TD was observed, as the TD increases both Q and U increase which is logic and agrees with basics of the heat transfer.

The temperature distribution for different aspect ratios at $\theta=0$ and TD = 90 K are shown in Fig. 6. Using the same Eq. (15), the constants a and b will depend on the aspect ratio variation as shown in table III.

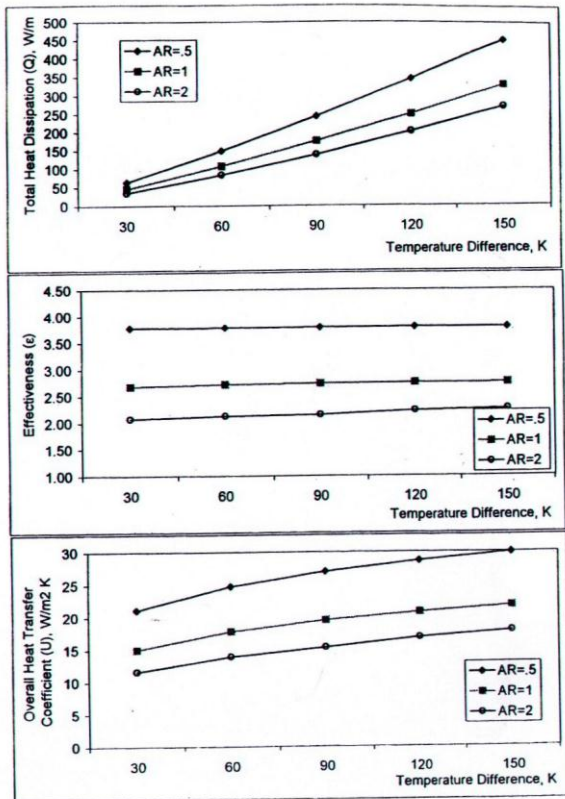


Fig. 5. Effect of aspect ratio (AR) for different temperature difference on the heat transfer form L-Shape having inclination angle=0 deg.

C. General Correlations

One of the objectives of the present work is to give the designer simple and accurate tools to calculate the heat transfer rates from different steel structure shapes.

That is why, the correlations in tables II and III were analyzed extensively by using different techniques. Hence, the general correlations representing all the results are:

a) Effect of inclination angle:

$$U = 6.9 \Delta t^{0.23} (1.01 + 0.41 \cos \theta - 0.42 \cos^2 \theta), 0 \leq \theta < \pi/2 \dots (16)$$

$$U = 6.9 \Delta t^{0.23} \frac{0.86 - 0.82 \cos \theta}{1 + 1.51 \cos \theta + 0.56 \cos^2 \theta}, \pi/2 \leq \theta < \pi \dots (17)$$

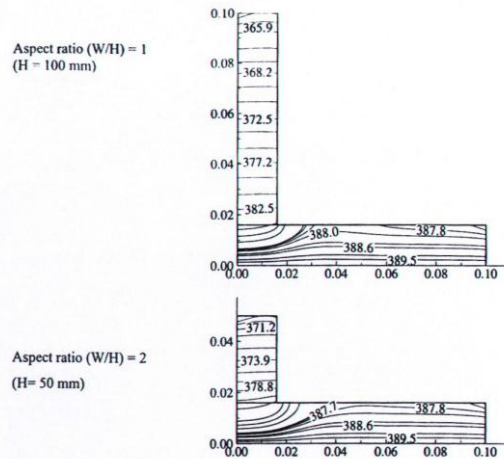


Fig. 6. Temperature contours across the L-shape sections for different aspect ratios ($\theta=0$, TD=90 k, $T_b=390$ K, $T_a=300$ K, $k=60.5$ W/m K, $W=0.1$ m and $t=0.016$ m).

TABLE III. Constants of Eq. (15) for various aspect ratios (AR).

AR	A	b
0.5	10.46	0.21
1	6.9	0.23
2	4.6	0.27

b) Effect of aspect ratio

$$U = 6.9 \Delta t^{0.23} (1.96 - 1.34AR + 0.38AR^2), 0.5 \leq AP \leq 2 \dots (18)$$

These general correlations can be used within the studied parameters stated in this section. They can be used to evaluate each steel structure shape from the heat-transfer point of view.

D. Comparison between Different Steel Structure Shapes (L, U and T)

Modifications of the present program designed to solve the heat transfer characteristics in L-shape were done to solve half-U and half-T geometry. Figure 7 shows the idea of these modifications. Finally to get the total heat transfer from certain U or T shape, the half-shape must be multiplied by 2. However, the overall heat transfer coefficient correlations can be used directly.

Figure 8 shows the heat transfer rates, effectiveness and overall heat transfer coefficient for different shapes and temperature difference at $\theta=0$ or π . The other parameters have the same values (AR=1, H=W=100 mm. t=16 mm, k=60.5 w/m K and $T_a=300$ K). It is clear from these figures that the L-shape has the highest heat transfer rates compared with half-U and half-T and the lowest one is half-T (where the insulated surface is bigger, as shown in figure 7). For U-shape and T-shape, the same heat transfer trends similar to the L-shape were observed (with respect to the variation of θ and TD).

Figure 9 shows the temperature distribution for different shapes at AR=0, $\theta=\pi$. It is clear in these figures that the heat flow from the insulated surface is equal to zero. Using

Equation (15), simple engineering correlations were given for each case and reported in table IV.

TABLE IV. Constants of Equation (15) for different steel structure L, U and T shapes.

Shape	θ	a	b
L	0	6.9	0.23
U		6.26	0.23
T		4.91	0.23
L	π	5.62	0.23
U		4.98	0.23
T		3.63	0.23

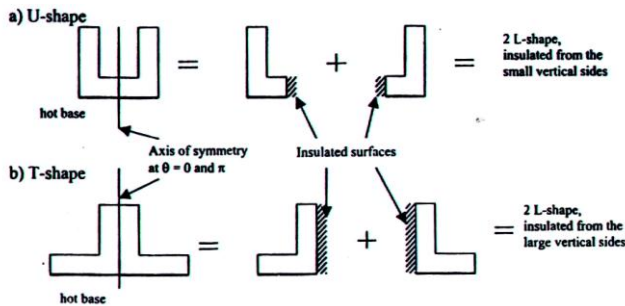


Fig. 7. Simulation of U and T-shapes with respect to L-shape.

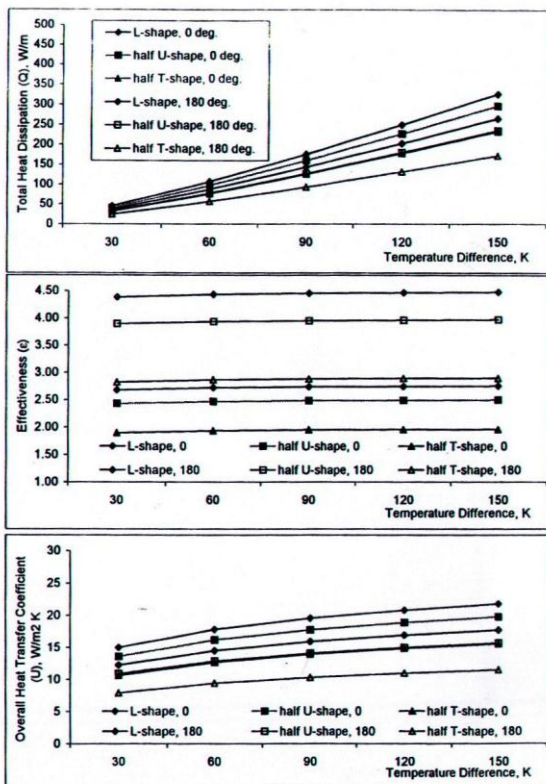


Fig. 8. Comparison between heat transfer from different steel structure shapes for different temperature and difference inclination angles.

E. Comparison with Previous Work

The available previous work taking the conduction and free convection for steel structure section into consideration is that of Riad [18]. He studied the heat transfer from I-beams experimentally and numerically (using finite difference and finite element techniques). Fair agreement between both

results was reported. The heat flow vectors were made by using the ready-made computer package "FEHT" [19]. However, in the present finite difference analysis, additional subroutine was written to calculate the heat flow vectors in each steel structure shape (L, U and T). The same heat flow trends (temperature contours and heat flow vectors) were observed in the horizontal and vertical webs of I-beam and half T-shape.

IV. CONCLUSIONS

Finite-difference technique and computer program were established to get the heat transfer (by conduction and natural convection at surfaces) from different steel structure shapes (L, U and T). The program is capable of obtaining the temperature and heat flow distribution at any inclination angle (0- π), temperature difference (30-150K) and aspect ratio (0.5-2). Samples of the program results-were plotted in graphs and a relation for each case was reported, Moreover, general correlations Eqs. (16-18), were driven. These correlations enable the designers to calculate simply and accurately the overall heat transfer coefficient at different operating and geometrical conditions of such shapes.

It was found that the rate of heat transfer increases as the inclination angle increases except at $\theta=\pi/2$ and π , which have lowest heat transfer rates. Also, the rate of heat transfer increases as the aspect ratio decreases and the temperature difference increase. In general, the change of effectiveness (from 2 to 4.5) is dependent only on the change of inclination angle and/or aspect ratio, L-shape has the highest overall heat transfer coefficient and the lowest one is T-shape, under the same conditions.

V. LIST OF SYMBOLS

- A=Surface arm, m²
- AR=Aspect ratio, the ratio between the L-shape width and height
- a,b=Constants
- h=Coefficient of heat transfer by convection, W/m²K
- k=Thermal conductivity of the plain carbon steels = 60.5 W/MK
- m,n=Axial and vertical grid indices in x and y directions
- Q=Heat transfer finni the shape per unit length in third direction, W/m
- T=Temperature, K
- T_D=Temperature difference (=T_b - T_a), K
- T_a=Ambient temperature, K
- T_f=Mean film temperature, K
- T_w=Mean wall temperature, K
- T =Web thickness of the L-shape in INCH
- U=Overall heat transfer coefficient, U=Q/(A_b(t_b-t_a)), W/m² K
- W,H=Width and height of the L-shape in meter
- β =Coefficient of volumetric thermal expansions = 1/T_f, 1/K
- Δt =Temperature difference, K
- A_x,A_y= Axial and vertical distance between successive nodes, m
- C=Effectiveness

θ =Inclination angle of L, U or T-shapes with respect to horizontal axis, degree

Heat transfer dimensionless groups

Gr=Grashof number,

No=Nusselt number,

Pr=Prandtl number

Ra=Rayleigh number

Subscripts:

B=base surface of the steel structure shape

H=horizontal surface

I=point number i in the grid

v=vertical surface

REFERENCES

- [1] J. J. J. Chen, C. C. Wei, and A. D. Ackland, "A water-model study of the ledge heat transfer in an aluminum cell," *Light Metals*, TMS, pp. 357, 1996.
- [2] A. M. Riad, "Heat Transfer from I-Beams," M.Sc. Thesis, Mechanical Power Engineering Dept., Faculty of Engineering, Cairo University, 2001.
- [3] Abbass Z. Salman, Roshen Tariq Ahmed, "The comparison analysis of fixed pitch angle wind turbine that of a double output induction generator," *National Renewable Energies Conference and Their Applications*, pp. 96-107, University of Technology, Baghdad, IRAQ, 2013.
- [4] S. A. Klein, W. A. Beckman, and G. E. Mayers, "Finite element heat transfer analysis," FEHT, F-Chart Software, Middleton, WI, USA, 1996.
- [5] D. Angimsa, and R. L. Mahajan, "Natural convection from L-Shaped comers with adiabatic and cold isothermal horizontal walls," *ASME Journal of Heat Transfer*, vol. 115, pp. 149-157, 1993.
- [6] C. Rodighiero, and L. M. de Socio, "Some aspects of natural convection in a cortices," *ASME, Journal of Heat Transfer*, vol. 105, pp. 212-214, 1993.
- [7] C. Balnji and S. P. Venkateshan, "Natural convection in L corners with surface radiation and conduction," *ASME, Journal of Heat Transfer*, vol. 118, issue 1, pp. 222-225, 1996.
- [8] Abbass Z. Salman, "The aerodynamical and structural analysis of wind turbine blade for fatigue prediction," *Journal of Natural Sciences Research*, vol. 7, issue 8, pp. 1-15, 2017.
- [9] Paolo Luchini, "Analytical and numerical solutions for natural convection in a corner," *AIAA Journal*, vol. 24, no. 5, pp. 841-848, 1986.
- [10] K. Hassan and S. A. Mohamed, "Natural convection from isothermal flat surfaces," *Int. Journal of Heat Mass Transfer*, vol. 13, issue 12, pp. 1873-1886, 1970.
- [11] S. W. Churchill, and H. H. S. Chu, "Correlating equations for laminar and turbulent free convection from a vertical plate," *Int. Journal of Heat Mass Transfer*, vol. 18, issue 11, pp. 1323-1329, 1975.
- [12] Mahdi A. Abdul-Hussain and Roshen T. Ahmed, "Connect the wind farms to the electrical grid and indicate their effect on improving the characteristics of the network", *International Research Journal of advanced Engineering and Science*, vol. 3, issue 1, pp. 45-48, 2018.
- [13] J. R. Lloyd and W. R. Moranv, "Natural convection adjacent to horizontal surface of various planforms," *J. Heat Transfer*, vol. 96, issue 4, pp. 443-447 1974.
- [14] D. W. Hatfield and D. K. Edwards, "Edge and aspect ratio effect on natural convection from the horizontal heated plate facing downwards," *Int. J. Heat Mass Transfer*, vol. 24, issue 6, pp. 1019-1024, 1981.
- [15] T. Fujii, and H. Hours, "Natural convection heat transfer from a plate with arbitrary inclination," *Int. L. Heat Mass Transfer*, vol. 15, issue 4, pp. 755-764, 1972.
- [16] Roshen Tariq Ahmed, Waleed Khalid Ibrahim, Ayad Mahmoud "Salman, using personal computer for vibration measurements and rotor balancing", *Journal of Engineering*, vol. 16, pp. 5149-5129, University of Baghdad, 2010.
- [17] J. P. Holman, *Heat Transfer*, McGraw-Hill International (UK) Limited, 76 Edition in SI Units, 1992.
- [18] Abbass Z. Salman, "Fatigue live for smooth specimen and microcracks growth model in torsion", *Engineering and Technology Journal*, vol. 24, issue 1681-6900, University of Technology, 2005.
- [19] D. A. Anderson, J. C. Tannehill, and R. H. Pletcher, *Computational Fluid Mechanics and Heat Transfer*, Hemisphere Publishing Corp., USA, 1994.